POLYPUBLIE
Polytechnique Montréal

POLYTECHNIQUE MONTRÉAL
UNIVERSITÉ D'INGÉNIERIE

Titre: Title:	Improving the re-use potential of reactive waste rock using sieving: a laboratory geochemical study
Auteurs: Authors:	Karine Sylvain, Thomas Pabst, & Isabelle Demers
Date:	2024
Type:	Article de revue / Article
Référence: Citation:	Sylvain, K., Pabst, T., & Demers, I. (2024). Improving the re-use potential of reactive waste rock using sieving: a laboratory geochemical study. Environmental Science and Pollution Research, 17 pages. https://doi.org/10.1007/s11356-024-34679-8

🔓 Document en libre accès dans PolyPublie
Open Access document in PolyPublie

URL de PolyPublie: PolyPublie URL:	https://publications.polymtl.ca/59189/
Version:	Version officielle de l'éditeur / Published version Révisé par les pairs / Refereed
Conditions d'utilisation: Terms of Use:	CC BY-NC-ND

📄 Document publié chez l'éditeur officiel
Document issued by the official publisher

Titre de la revue: Journal Title:	Environmental Science and Pollution Research
Maison d'édition: Publisher:	Springer
URL officiel: Official URL:	https://doi.org/10.1007/s11356-024-34679-8
Mention légale: Legal notice:	This article is licensed under a Creative Commons Attribution-NonCommercial-NoDerivatives 4.0 International License, which permits any non-commercial use, sharing, distribution and reproduction in any medium or format, as long as you give appropriate credit to the original author(s) and the source, provide a link to the Creative Commons licence, and indicate if you modified the licensed material. You do not have permission under this licence to share adapted material derived from this article or parts of it. The images or other third party material in this article are included in the article's Creative Commons licence, unless indicated otherwise in a credit line to the material. If material is not included in the article's Creative Commons licence and your intended use is not permitted by statutory regulation or exceeds the permitted use, you will need to obtain permission directly from the copyright holder. To view a copy of this licence, visit http://creativecommons.org/licenses/by-nc-nd/4.0/.

RESEARCH ARTICLE

Improving the re-use potential of reactive waste rock using sieving: a laboratory geochemical study

Karine Sylvain[1,2] · Thomas Pabst[1,3] · Isabelle Demers[2]

© The Author(s) 2024

Abstract

Stockpiles containing sulfide minerals are subject to oxidation reactions when exposed to atmospheric conditions, which can result in the formation of acid mine drainage (AMD). Reactive waste rock has limited re-use potential due to the contamination risk associated with the generated drainage water. The re-use of reactive waste rock could lead to a significant reduction in the volume of waste rock as it mitigates the environmental impact of mine waste deposition. Acid mine drainage generation rate depends on sulfide weathering kinetics which are controlled by many parameters such as the mineralogy and the particle size. Fine fractions of waste rock have higher specific surface areas and degree of liberation of sulfides, resulting in greater reactivity than the coarse fractions. The objective of this research was therefore to evaluate the potential of re-use by controlling particle size using the sieving method. Two different potentially acid-generating waste rocks were divided into six fractions and subjected to both static and kinetic tests. Prediction of the geochemical behavior using static test did not consider the liberation of the minerals, and the long-term prediction was therefore overestimated. Results of the kinetic columns showed there was less oxidation of the sulfide minerals in the coarse fractions than in the fine fractions. Additionally, the distribution of sulfidic minerals and neutralizing minerals with particle size is influencing the potential of the re-use of the reactive waste rock.

Keywords Waste rock geochemistry · Acid mine drainage (AMD) · Waste rock valorization · Kinetic test · Mine waste management · Circular economy

Introduction

Waste rock is non-economic material produced by blasting and typically stored in stockpiles that can reach several dozens of meters in height and exceed a hundred hectares in surface (Amos et al. 2015; Vriens et al. 2020a,; Dimech et al. 2022). These piles can contain hundreds of millions of cubic meters of waste rock, with particle sizes ranging from micrometers to meters (Aubertin 2013). Stockpiles are heterogeneous structures that are mainly controlled by the construction method (e.g., end-dumping, push-dumping), the mine sequencing, and the physical and chemical composition of the waste rock (Fala et al. 2003, 2013; Lapakko et al. 2006; Lahmira et al. 2017). This internal heterogeneity poses significant challenges for waste rock management, particularly regarding the geochemical stability (Lahmira et al. 2017; Martin et al. 2017).

Stockpiles are often left exposed to atmospheric conditions until their reclamation at mine closure (Molson et al. 2005; Amos et al. 2015; Vriens et al. 2020a). The presence of sulfide minerals can therefore lead to the generation of acid mine drainage (AMD) (Blowes et al. 2014; Amos et al. 2015), characterized by low pH and high concentrations of dissolved metal(loid)s and sulfate (Amos et al. 2015). The intensity of AMD generation of waste rock depends on several factors such as the transport mechanism of gas and water (Chi et al. 2013; Lahmira et al. 2014; Bao et al. 2020), mineralogical composition (Parbhakar-Fox et al.

✉ Karine Sylvain
karine.sylvain@uqat.ca

1 Research Institute On Mines and Environment (RIME) Polytechnique Montreal, Rouyn-Noranda, QC, Canada

2 Research Institute On Mines and Environment (RIME), Université du Québec en Abitibi-Témiscamingue, Rouyn-Noranda, Québec, Canada

3 Present Address, Norwegian Geotechnical Institute (NGI), Oslo, Norway

🙋 Springer

2013), particle size distribution and specific surface area (Smith et al. 2013a, b; Erguler and Kalyoncu Erguler 2015), climatic conditions (Neuner et al. 2013; Vriens et al. 2019a, b), and microbiological mechanisms (Nordstrom et al. 2015; Blackmore et al. 2018).

Waste rock is traditionally stored on-site indefinitely in the absence of technical ability to re-use (Vriens et al. 2020). Reclamation techniques aim to reduce the risk of AMD, but they are often implemented at the end of mining operations which can involve the need to manage drainage water. Although management methods such as desulfurization can effectively reduce the risk of AMD for tailings regarding their deposition (Benzaazoua and Kongolo 2003; Alam and Shang 2012; Ait-Khouia et al. 2021), flotation processes are limited by particle sizes (Derycke et al. 2013) and therefore not applicable to waste rock. Furthermore, waste rock piles are very large structures which make them difficult to manage, and the reclamation is complex because of their steep slope, the vegetation establishment, and the control of the water balance (Martin et al. 2017).

Large quantity of waste rock can be strategically managed by combining economic efficiency with environmental sustainability using a circular economy approach (Aznar-Sánchez et al. 2018). Non-acid-generating waste rock can be re-used for various applications such as the construction of mine haul roads (Laverdière et al. 2023), dam structures, drainage inclusions (Saleh-Mbemba et al. 2019), backfilling (Li et al. 2019), and cover systems for the reclamation of tailing storage facilities (Kalonji Kabambi et al. 2017; Pabst et al. 2017). The re-use of waste rock reduces both the volume deposited on the site and the needs of material, in which extraction can have significant environmental and economic impacts (Tayebi-Khorami et al. 2019). However, waste rock is often acid generating, which may prevent their re-use.

A promising approach involves segregating and sieving (removing) some fractions of the waste rock to control its reactivity, a method demonstrated for uncertain to non-acid-generating waste rock by Elghali et al. (2018, 2019). This method is based on the principle that finer particles exhibit greater oxidation rate in comparison with the coarser fractions (Hollings et al. 2001) and higher contaminant release rates (Lapakko et al. 2006; Erguler et al. 2014). This can be attributed to the specific surface area of the waste rock, which is inversely proportional to particle size, but also to the specific surface area of the sulfide minerals (Hollings et al. 2001; Lapakko et al. 2006; Erguler and Kalyoncu Erguler 2015). Additionally, the proportion of sulfide minerals exposed to oxidation is higher in the fine samples compared to the coarse samples, due to different degrees of liberation (Erguler and Kalyoncu Erguler 2015).

Specifically, particle size smaller than 0.25 mm contributed substantially (i.e., more than 80%) to oxidation and neutralization reactions in waste rock from various mining sites, such as the Aitik Cu mine (Strömberg and Banwart 1999) and the Hillsboro mining district in Sierra Country (Munroe et al. 1999). Other findings showed that fine fractions (< 2.5 mm) in waste rock can contain a higher quantity of sulfide minerals (Smith et al. 2013a, b), often in liberated form (Elghali et al. 2018), and thus can be more reactive. These findings underline the significance of targeted particle size removal as an effective means of managing acid-generating waste rock.

Waste rock reactivity is impacted by high physico-chemical variability (Marescotti et al. 2010; Lahmira et al. 2016; Wilson et al. 2022) and their mineralogy (Smith et al. 2013a, b; Vriens et al. 2019a, b; St-Arnault et al. 2020). Determining the potential for waste rock re-use and selecting the fraction are site-specific. The objective of this research was to evaluate the contribution of different fractions of waste rock to acid generation and to determine the fraction size that could be re-used without environmental risks. Effective management of reactive waste rock could indeed reduce the contaminant load, and thereby contribute to the development of novel sustainable mine waste management practices. Two different potentially acid-generating waste rocks with different mineralogies were tested in the laboratory. A total of 12 weathering column tests were performed to assess the geochemical behavior of various waste rock fractions.

Materials and methods

Site description and waste rock sampling

Two waste rocks from two different gold mine sites located in the Abitibi-Temiscamingue region, in Canada, were studied in this research: Canadian Malartic (open-pit mine) and LaRonde (underground mine). Around 400 kg of waste rock was sampled from each site in the waste rock piles and sent in hermetic barrels to Polytechnique Montreal laboratory. The selection of the maximum size fraction was guided by practical considerations, as removing large boulders and large particles is a common practice when repurposing waste rock for construction, such as in mine hauls road (e.g., maximum particle size of 40 mm; Thompson et al. 2019) or cover systems (Kalonji Kabambi et al. 2017). Waste rock was truncated to a maximum particle size of 37.5 mm to respect a ratio of 8 between the largest particle size and the diameter of the laboratory columns. Samples were dried in the laboratory and homogenized using the quartering technique (ASTM C702 2018). Subsequently, samples were stored in hermetically sealed buckets prior to testing.

Canadian Malartic

Canadian Malartic mine is one of the largest open-pit gold mines in Canada and is located in the city of Malartic, Quebec (Helt et al. 2014). The operation started in 2011, and most of the produced waste rock is deposited in the waste rock pile which currently has a height of 60 m. The total amount of waste rock generated by the end of the operations is estimated to be approximately 624 Mt, and the final stockpile is expected to cover a surface of approximately 264 hectares (Mine Canadian Malartic 2020). Canadian Malartic mine is re-using the waste rock for different purposes, such as tailings dam construction. A portion of the waste rock was repurposed and incorporated as inclusions in the tailing impoundment (James et al. 2013). Large-scale test benches have been constructed to assess the potential for re-use of non-reactive waste rock as cover material (Mine Canadian Malartic 2020). However, the long-term prediction of most of the waste rock regarding acidification is uncertain. Currently, the reclamation plan for the waste rock pile includes the installation of a low permeability layer and a topsoil to enhance vegetation growth.

LaRonde

The LaRonde complex is a gold-rich volcanogenic massive sulfide deposit exploited since 1988 which also produces copper and zinc. The LaRonde complex hosts five historic underground mines and a number of small open pits. The complex comprises the LaRonde mine and the LaRonde Zone 5 mine (LZ5). The samples were collected from the LaRonde mine sector in this study. At the LaRonde mine, a large part of the produced waste rock is re-used for backfilling the underground mine, and the rest ($\approx$1 Mt or 1.4 Mm^3; Agnico Eagle 2021) is stored in two piles. The mine is planning to re-use most of the waste rock to stabilize the access and the slopes of the tailing storage facility and for its reclamation (Agnico Eagle 2021). Identifying which fraction generates more AMD could be beneficial for enhancing the planning and the design for re-use.

Physical properties

Waste rock samples (400 kg for Canadian Malartic and LaRonde) were separated in 14 size fractions in the laboratory using mechanical sieving (37.5, 25, 19, 14, 10, 4.75, 3.35, 2.36, 2.0, 1.4, 1.0, 0.85, 0.425, 0.25, and 0.075 mm; ASTM D6913 2021). The results were fitted using the Fredlund model (2000). The particle size distribution of LaRonde (LR) and Canadian Malartic (CM) waste rock samples collected at a maximum particle size of 37.5 mm were similar with a characteristic diameter $d_{10} = 0.1$ mm (dx corresponding to x% passing on the particle size distribution curve) and a coefficient of uniformity $C_u = d_{60}/d_{10} \approx 130$ (Fig. 1).
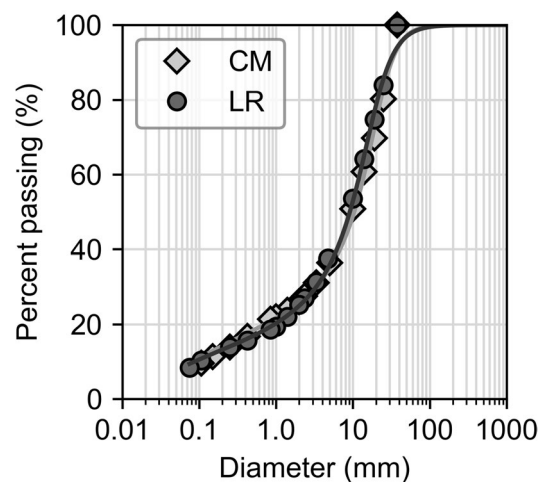
Fig. 1 Particle size distribution of LR (circle) and CM (diamond) waste rock samples. PSD curve is described using Fredlund (2000) model

The specific gravity of particles smaller than 4.75 mm was measured using the D854 ASTM (2014) standard, and the specific gravity of particles larger was measured using C127 ASTM (2015). Higher specific gravity typically indicated greater sulfide mineral contents as those minerals have a higher density than the gangue (Amar et al. 2020). CM waste rock specific gravity was between 2.69 and 2.76 (Fig. 2). LR specific gravity tended to decrease with increasing particle size, varying from 3.00 in the fine fraction (< 1 mm) to less than 2.90 in the coarse fraction (> 1 mm).

Mineralogical and geochemical characterization

The total sulfur and carbon contents (%S and %C) were analyzed using an induction furnace (ELTRA CS-2000). Fourteen particle size fractions (< 0.25, 0.25, 0.425, 0.85, 1.0, 1.4, 2.0, 2.36, 3.35, 4.75, 10, 14, 19, 25, 37.5 mm) for each waste rock were analyzed. Specifically, the fine fraction [0; 4.75 mm] of the waste rock was subdivided into four distinct fractions for further characterization and testing. Each sub-fraction was separated by approximately 1-mm intervals and designated as C1 to C4. The larger particle fraction [4.75; 37.5 mm] was labeled as fraction C5, and the entire range of fractions [0; 37.5 mm], i.e., the original material, was referred to as C6. The mineralogical semi-quantification of the major mineral phases ($\pm$1% precision) was determined by X-ray diffraction (XRD) using the Rietveld method for the weathering column fractions (C1 [0; 1 mm], C2 [1.00; 2.36 mm], C3 [2.36; 3.35 mm], C4 [3.35; 4.75 mm], C5 [4.75; 37.5 mm]).

Mineralogy was reconciled using bulk chemical composition by inductively coupled plasma atomic emission spectrometry (ICP-AES) following a four-acid digestion with

Fig. 2 Specific gravity of CM and LR by fractions (with standard variations) and calculated for the total fraction (dashed bar)
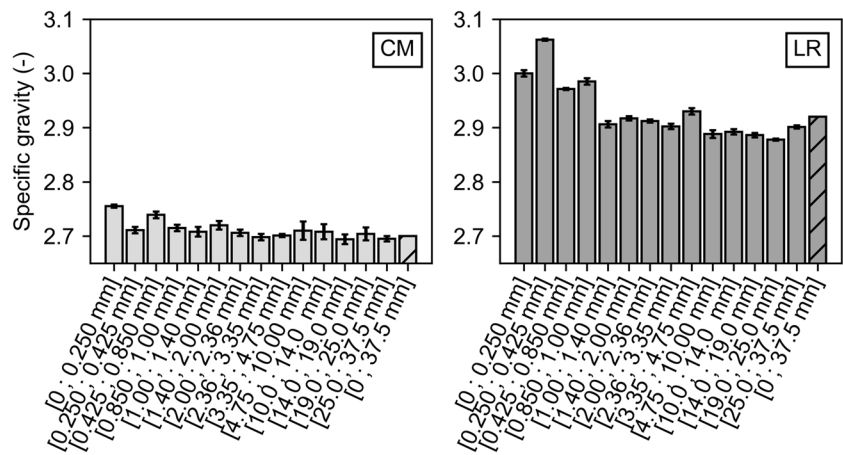
$HNO_3/Br_2/HF/HCl$ and induction furnace (%*S* and %*C*). The reconciliation was done using the main elements (Al, Ba, C, Ca, Cu, Fe, K, Mg, Mn, Na, S, Zn, Ti), and the root-mean-square deviation (RSMD) was calculated for the reconciliated XRD with ICP-AES results. The generalized reduced gradient method was used to minimize the RSMD until the solver reached a solution. A constraint of ±3% of XRD values was considered in the solver to reach the solution, but manual adjustments were exceptionally made for certain minerals. The chemical composition and the mineralogy of the total fraction C6 [0; 37.5 mm] were then reconstituted by calculating the weighted average of C1 to C5 results.

Acid base accounting

Acid base accounting (ABA) tests were performed for the weathering column fractions C1 to C6. The neutralization potential (NP) was calculated based on the total carbon content by the standard carbonate NP (CNP) method assuming carbon solely originated from $CaCO_3$ (Price 2009). The acid-generating potential (AP) was calculated based on the total sulfur content. Mineral reconciliation was used to

correct the AP by approximating the contribution of S from sulfide minerals and excluding consideration of S contributed by sulfate minerals. The neutralization potential ratio (NPR = NP/AP and NPR = NP/AP) was then calculated to evaluate the potential of acid generation of the three tested waste rocks. The material was considered potentially acid generating (PAG) if NPR < 1, non-PAG if NPR > 2, and uncertain for NPR between 1 and 2 (Price 2009).

Weathering column tests

A total of eight small weathering columns (i.e., four for each waste rock) and four larger columns (i.e., two per waste rock) were set up in the laboratory (Fig. 3). Each column contained different and complementary fractions: C1 [0; 1 mm], C2 [1.00; 2.36 mm], C3 [2.36; 3.35 mm], C4 [3.35; 4.75 mm], C5 [4.75; 37.5 mm], and the total fraction C6 [0; 37.5 mm]. The larger columns were set up to ensure a ratio of at least 8 between the column's inner diameter and the maximum particle size diameter and limit border effects (Peregoedova 2012). One kilogram of waste rocks

Fig. 3 Configuration and experimental setup of weathering small column tests C1 to C4 and the large column tests C5 and C6
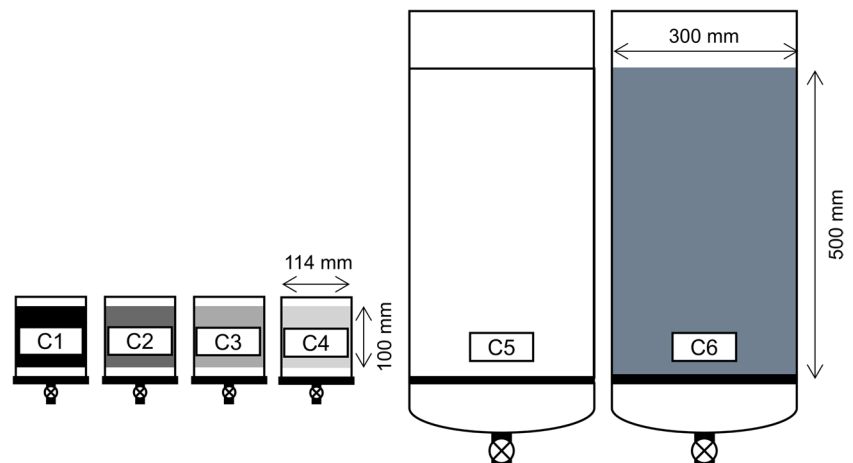
was placed dry and loose in the small columns at a porosity of around 0.4. For the large columns, 55.3 kg was placed dry ($w = 3\%$) and loose at a porosity varying between 0.25 and 0.41 (depending on the particle size distribution).

The columns were left open and exposed to the atmospheric conditions in the laboratory. Multiple wetting–drying cycles were applied to all the columns. Cycle duration varied with the size of the columns and the observed geochemical behavior. Twenty cycles for a duration of 140 to 175 days were applied to the small columns, while the larger column tests were conducted for 15 cycles of around 30 days and lasted 461 days. At the beginning of each wetting–drying cycle, distilled water (0.40 L for the small columns, i.e., a solid/liquid ratio of 0.40, and 19 L for the larger columns, i.e., a solid/liquid ratio of 0.35), was added on the top of the columns and left in contact with the samples for 4 h. The distilled water has a pH between 5.5. and 6.0 due to the equilibrium with atmospheric CO_2. The valve at the bottom was subsequently opened to collect the leachates.

Leachates were analyzed for pH, redox potential (ORP), electrical conductivity (EC), and temperature using Hanna HI5222 Benchtop Meter. Alkalinity and acidity were determined by manual titration using 0.02 N H_2SO_4 and 0.02 N NaOH. The composition of the leachate (Al, As, Ba, Be, Bi, Ca, Cd, Co, Cr, Cu, Fe, K, Li, Mg, Mn, Mo, Na, Ni, Pb, S, Se, Si, Sr, Te, Ti, and Zn) was analyzed by ICP-AES (Perkin Elmer Optima 3100 RL) after filtration (0.45 μm) and acidification (50% volumes/volumes HNO_3). Sulfate concentrations were determined by turbidimetric method using Hach DR3900 (Clesceri et al. 1998) and were compared to S concentrations from ICP-AES. A blank was analyzed for each analysis. Duplicates were analyzed at a frequency of one randomly selected sample for every ten samples. Sulfate calibration was performed using a working set of 0, 10, 30, 50, and 70 mg/L solution prepared by using a standard solution of 100 ± 1 mg/L. Cumulative normalized loadings (mg/kg) of sulfate and other elements were calculated, and the release rate was determined using linear regression after five cycles. A geochemical speciation model (Visual MINTEQ 4.05) was used to assess the potential distribution of elements among different phases (solid, aqueous, or gaseous phases) and to investigate chemical equilibrium and potential precipitation of secondary minerals in the collected leachates (Plante et al. 2010).

Results

Preliminary chemical characterization

The 14 particle size fractions for each waste rock were analyzed for sulfur content and carbon content. All waste rocks showed a significantly greater sulfur content than carbon contents. The specific gravity results were generally correlated with the sulfur content results for LR waste rock (Pearson correlation coefficient (PCC); $\rho = 0.87$; p-value $= 6E - 5$), but no correlation was observed between specific gravity results and the sulfur content for CM (PCC < 0.1; p-value > 0.7).

The sulfur content of the entire waste rock sample [0; 37.5 mm] was 1.8%. Sulfur content in CM waste rock was relatively uniform and around 2% ($\pm 1\%$) in all fractions, with slightly greater sulfur content in the fine fractions [0; 0.250 mm] and [0.250; 0.425 mm] with 2.3% and 2.7%, respectively (Fig. 4a). These two fractions constituted only 16.8% of the total mass of the sample (Fig. 1) and accounted for 21.2% of sulfur mass in the CM waste rock (Fig. 5a). Sulfur in CM waste rock was primarily concentrated in the coarse fraction (> 4.75 mm), constituting around 64% of the total sulfur content (Fig. 5a). The carbon content was relatively uniform and around 0.5% in all fractions except for fraction [0; 0.250 mm] where $\%C = 0.9\%$, suggesting a greater neutralization potential of the finest fraction. However, this fraction represented only a small amount of the entire waste rock, and most of the carbon (57%) was in fact associated with the coarse fraction > 4.75 mm (Fig. 5b). In LR waste rock (Fig. 1), the whole sample [0; 37.5 mm] sulfur content was 3.6%.

Fig. 4 Sulfur and carbon content of (**a**) CM and (**b**) LR
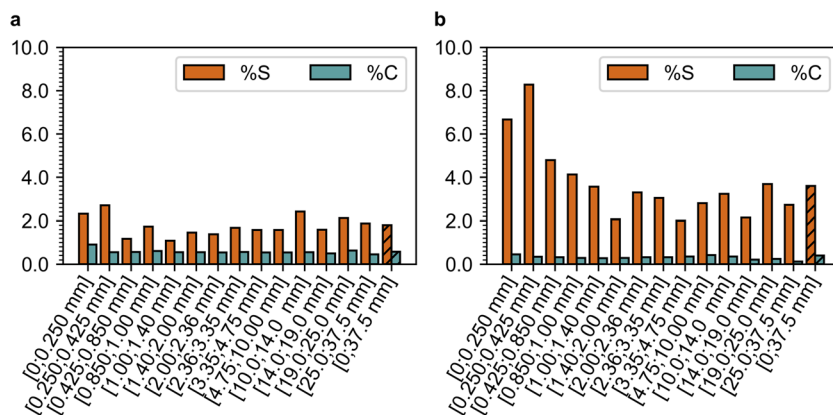
Fig. 5 Particle size distribution normalized to (**a**) total %*S* and (**b**) total %*C*. For example, 40% of the total sulfur content is passing the sieve size 2 mm for LR
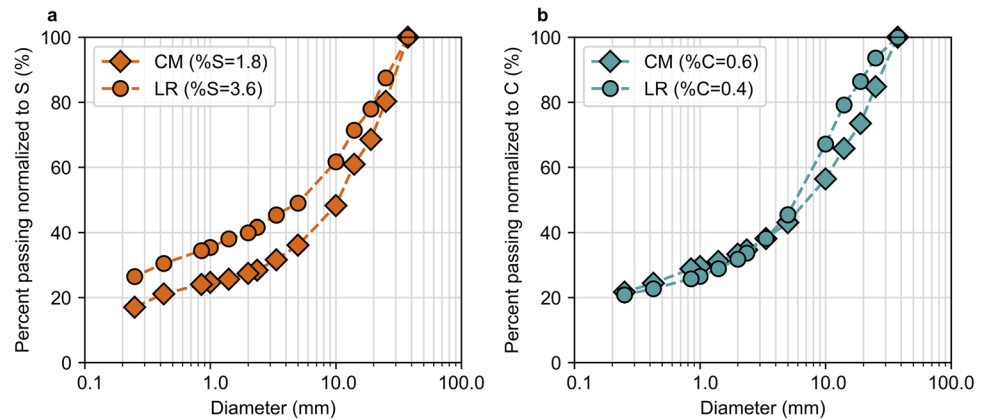
Sulfur was enriched (48.9%; Fig. 5b) in the fraction passing the sieve size of 4.75 mm, and sulfur content tended to decrease with increasing particle size (Fig. 4b). For example, sulfur was around 6 to 8% in the smallest fractions [0; 0.250 mm] and [0.250; 0.425 mm]. Sulfur content was less than 3% in the fractions greater than 1.00 mm (Fig. 4b). No significant variation of the carbon content was observed in the different fractions of LR waste rock which was generally between 0.2 and 0.4%. The majority (54.6%) of the carbon was contained in the coarse fractions greater than 4.75 mm (Fig. 5b).

Both waste rocks showed a similar particle size distribution. The fraction [0; 4.75 mm] constituted 38% of the sample mass for both waste rocks. However, significant differences in S distribution were observed. In LR waste rock, 49% of the total sulfur was contained in the [0; 4.75 mm], while in CM waste rock, 36% of the total S content was contained in the same fraction. Sieving the fine fraction of LR could enable the separation of the more

reactive fraction, which contained half of the total sulfur from the less reactive coarse fraction.

Static tests results

CM waste rock

Total sulfur concentrations in fractions C1 to C5 varied from 1.1 to 1.9% (Fig. 6a). Fe and S concentrations in C6 were 2.6% and 1.8% respectively. Fe and S concentrations were slightly lower in the fraction C2 [1.00; 2.36 mm], with 2.5% and 1.1%, respectively, but there was no clear trend with particle size (Table A.1). Based on XRD quantification results, pyrite (FeS_2) was the primary sulfide mineral, and no other sulfide mineral was detected by XRD analysis. Mineralogical reconciliation of XRD, ICP-AES, and induction furnace measurements (RSMD < 0.1; see "Methodology section" for details) indicated a concentration of pyrite of 2.7% in the total fraction C6, with a maximum of 3.3% in fraction C1
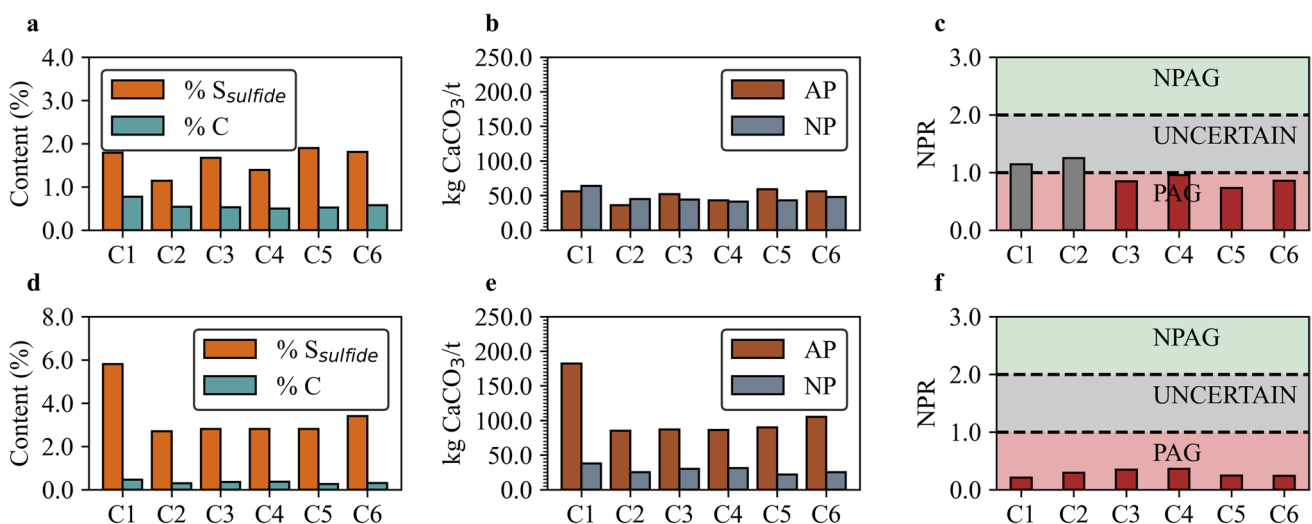
Fig. 6 S and C content of the weathering columns, AP and NP and potential of acid generation for (**a**) S from sulfide minerals and C content of CM; (**b**) AP and NP of CM; (**c**) NPR of CM; and (**d**, **e**, **f**) same for LR

and a minimum of 2.1% in fraction C2. Zn concentrations (44 and 78 ppm) and Cu concentrations (28 to 42 mm) were limited, indicating a maximum chalcopyrite and sphalerite content of less than 0.01%. The concentrations of Ba, commonly associated with sulfur, ranged from 440 to 1434 mm, which may indicate the presence of some sulfate minerals such as barite ($BaSO_4 < 0.3\%$).

Carbon and calcium concentrations were 0.6% and 1.9% in the total fraction C6 and were relatively uniformly distributed in all fractions C1 to C5. C and Ca concentrations were slightly greater in the fine fraction C1 (0.7% and 2%, respectively; Table A.1). Calcite ($CaCO_3$) was identified as the primary carbonate mineral in CM waste rock, representing up to 4.7% in fraction C1. Some ankerite ($Ca (Fe, Mg, Mn) (CO_3)_2$) was also detected by XRD, particularly in column C5. Thus, mineralogical reconciliation suggested the presence of traces of ankerite ($< 0.5\%$) in all fractions (Table A.2). Silicates mainly consisted of quartz (27.5–38.0), plagioclase (37.0–41.8%), micas (5.3–6.5%), k-feldspar (4.5–5.5%), and chlorite (2.1–3.6%), which were relatively uniformly distributed (no trend with particle size).

AP was between 35 and 59 kg $CaCO_3$/t, and NP between 41 and 64 kg $CaCO_3$/t (Fig. 6b). AP was higher in the fine fraction C1 (55 kg $CaCO_3$/t) and in the coarse fraction C5 (59 kg $CaCO_3$/t). NP was slightly higher in finer fractions C1 [0; 1.00 mm] and C2 [1.00; 2.36 mm] than in coarser fractions. Overall, NPR of the whole waste rock (C6) was around 0.9, and the acid generation potential was therefore classified as PAG (Fig. 6c). However, fractions C1 to C2 were individually classified as uncertain (NPR between 1.2 and 1.3).

In summary, the sulfur content in CM waste rock fractions C1 to C5 exhibited some variation but was generally within the range of 1.1 to 1.9%, primarily in the form of pyrite. Carbon and calcium contents were consistent, in the form of calcite as the main carbonate minerals. The fine fraction C1 was enriched in carbonate minerals compared to the coarser fractions. The waste rock was classified as PAG, with some uncertainty in fractions C1 and C2.

LR waste rock

In LR whole waste rock (C6), Fe and S concentrations were 6.6% and 3.6%, respectively. Sulfur concentrations were the highest in the fraction C1 (6.3%; Fig. 6d). Elemental concentrations of Fe, Cu, and Zn in LR showed similar trends with greater concentrations in C1 and smaller (and relatively constant) concentrations in C2 to C5. For example, Fe content was 8.1% in C1, but between 6.0 and 6.3% in fractions C2, C3, C4, and C5. Pyrite (FeS_2) was the primary sulfide mineral in LR waste rock, with around 10% in C1 (10%), and between 4 and 5% in

C2 to C5. LR waste rock also contained traces of zinc (140 to 2453 ppm) and copper (160 to 977 ppm), which also tended to decrease as particle size increased. Mineralogical reconciliation (RMSD < 0.2) indicated the presence of traces of sphalerite, ZnS (0.1 to 0.4%), and chalcopyrite, $CuFeS_2$ (0.1 to 0.3%) in all fractions C1 to C5, although they were not detected by XRD results (most probably because of ~ 1% detection limit).

Carbon content was 0.4% in the whole waste rock fraction C6 [0; 37.5 mm], with similar values in fractions C2 to C5. Carbon content was slightly higher in concentrations in C1 (~ 0.5%). Calcite was identified as the main carbonate mineral, with the highest content in C1 (3%) and the lowest content in C5 (2%). Some ankerite was also detected by XRD in LR waste rock (< 0.7%).

Although Al, Mg, Ca, and Na contents were lower in fraction C1, no specific trend was observed in the XRD analysis for the non-sulfide gangue minerals within fractions C2 to C6. Silicates mainly consisted of quartz (31.4–41.0%), plagioclase (17–31%), micas (8.0–16.6%), chlorite (6.5–10.5%), and k-felspar (0.5–1.1%), which were showing slightly variation in the fine fraction C1 (Table A.2). Secondary minerals such as jarosite and gypsum were detected by XRD in C1, C2, C3, and C4, suggesting prior oxidation of the fractions < 4.75 mm. The highest jarosite content was observed in fraction C1 (1.5%), which is correlated with the observation of the highest K content (1.6%).

AP of LR waste rock was higher than the NP for all the fractions (Fig. 6e). The total fraction AP C6 (105 kg $CaCO_3$/t), which included 20% of the fine fractions C1, was in between C1 (182 kg $CaCO_3$/t) and C2 (85 kg $CaCO_3$/t). AP in LR waste rock increased with decreasing particle size, with the highest AP calculated in sample C1 (182 kg $CaCO_3$/t) followed by C2, C3, C4, and C5 (84–87 kg $CaCO_3$/t). Among all the fractions, the fine fraction C1 [0; 1.00 mm] had the highest NP (38 kg $CaCO_3$/t) compared to C2 to C6 (25 to 31 kg $CaCO_3$/t). However, NPR were lower than 0.4 for all fractions. Consequently, LR waste rock fractions were all classified as PAG (Fig. 6f).

In summary, sulfur content in LR waste rock fraction C1 was greater than in fractions C2 to C5, in the form of pyrite, but also, traces of chalcopyrite and sphalerite were detected. Carbon and calcium contents were consistent, in the form of calcite as the main carbonate minerals. The fine fraction C1 was enriched in carbonate minerals compared to the coarser fractions. LR waste rock was classified as PAG, regardless of the fraction size.

Weathering columns

As significantly larger sample masses were used in the large columns C5 and C6 than in the small columns C1 to C4, the results could not be compared directly (see more detailed analysis in the next section).

CM waste rock

The pH of the original material C6 [0; 37.5 mm] was slightly neutral to alkaline (between 7 and 8) in the first 280 days and then progressively decreased to reach pH 6.5 at the end of the test (Fig. 8a). pH in all CM waste rock small columns < 4.75 mm (C1 to C4) was initially slightly alkaline ~ 9, then decreased to 7.5 after nine cycles (59 days), and remained near neutral until the end of the tests (Fig. 7a). pH was also initially alkaline (pH = 8.5) in the large column C5 [4.75; 37.5 mm] during the first 250 days (nine cycles) but then decreased to 7 and remained neutral for the rest of the duration of the test (461 days; Fig. 8a).

Sulfate concentrations, which result from sulfide oxidation, were one order magnitude greater in the original material C6 [0; 37.5 mm] at 150 mg/L compared to the concentration in C5 [4.75; 37.5 mm] which was only 10 mg/L (Fig. 8b). Sulfate concentrations thus followed a downward trend as particle size increased: concentrations were highest in the fraction C1 during the test (40–460 mg/L), followed by C2 (7 to 40 mg/L) and by C3 and C4 with similar values (~ 10 mg/L; Fig. 7b).

Iron and zinc concentrations were relatively small in all CM column tests (below 0.5 mg/L; Fig. 7c and d). In the whole waste rock fraction C6, iron and zinc remained close to 0.1 mg/L (Fig. 8c and d). For the small column fractions C1 to C4, iron and zinc concentrations were below the detection limit after three to four cycles. The higher concentrations of iron and zinc in C1 to C4 during the initial three to four cycles suggested that oxidation products were dissolved, thus indicating that (limited) pyrite oxidation may have occurred prior to the laboratory testing. Iron and zinc are produced by the oxidation of sulfides and should therefore follow relatively well sulfate concentrations and the decreasing pH (Jambor et al. 2005). However, near-neutral pH may explain that most iron has precipitated in the form of oxyhydroxide minerals (Amos et al. 2015) and the high mobility of zinc at near-neutral pH can explain the concentrations in the leachate (Cravotta III 2008). Part of zinc concentrations could also be attributed to laboratory distilled water quality (average zinc concentration of 0.08 mg/L). Zn concentrations are total concentrations (Figs. 7d and 8d) and were not corrected for these elevated initial concentrations in the distilled water.

Calcium and magnesium mostly originated from the dissolution of carbonates and, possibly, to a lower extent, of silicates such as andesine or chlorite. Ca and Mg concentrations generally followed relatively well the variations of sulfates, i.e., an initial rapid and significant decrease during the first three cycles, their stabilization depending on the particle size, until the end of the test. Calcium and magnesium concentrations in the whole fraction C6 (~ 60 mg/L and ~ 7 mg/L) were half an order of magnitude greater than those in coarse fraction C5 (~ 12 mg/L and 1 mg/L; Fig. 8e and f). Calcium and magnesium concentrations are likely controlled by the fine fraction, with C1 (~ 70 mg/L and ~ 5 mg/L) exceeding concentrations in C2, C3, C4, and C5 (~ 10 mg/L and ~ 1 mg/L, respectively; Fig. 7e and f).

Overall, the pH in all columns was initially above 7 and gradually decreased to around 7 by the end of the tests. Neutral pH led to the precipitation of oxyhydroxides, therefore explaining the low concentrations of iron measured in the leachates. Sulfate concentrations were the highest in the fine fraction C1 [0; 1 mm] and in the whole fraction C6 [0; 37.5 mm], indicating the significant impact of the fine fractions on the concentrations of products coming from the oxidation processes. Calcium and magnesium concentrations followed a similar pattern, suggesting that fine fractions also contribute more to the neutralization processes than the coarse fractions.

LR waste rock

pH remained neutral during the first 190 days in the large columns C5 and C6, but a decreasing pH was observed from day 226 which reached slightly acidic values (~ 6.5) by the end of the experiment of the large columns (461 days; Fig. 10a). However, pH remained near neutral for the duration of the test (175 days) in the small LR columns C1 to C4 (Fig. 9a).

Sulfate concentrations decreased with increasing particle size. Sulfate concentrations were greater in the total fraction column C6 (200 mg/L) in comparison with the coarse fraction C5 (55 mg/L; Fig. 10b). Specifically, sulfate concentrations were one to two orders of magnitude greater in the column containing fine fraction C1 (1400 mg/L) than in the other small columns C2 to C4 (10 to 60 mg/L after day 20; Fig. 9b).

In the large columns C6 and C5, the trends of iron and zinc concentrations differed from sulfate concentrations (Fig. 10c and d). The concentrations of iron and zinc increased during the test, with higher levels observed in the coarse column C5 (0.9 mg/L and 2.1 mg/L, respectively) compared to C6 (0.1 mg/L and 1 mg/L, respectively). In the

large column C5, iron increased as the pH decreased and stabilized around 0.9 mg/L after 310 days (Fig. 10a). Iron concentrations were below the detection limit (< 0.006 mg/L) in all the small columns C1 to C4 after 120 days. Zinc concentration was on average 0.5 mg/L in column C1 (which is equal to the mean acceptable concentration of Quebec regulation) and 0.1 mg/L for C2, C3, and C4 (Fig. 9). The maximum concentration of 2 mg/L was observed in the large column C5 [4.75; 37.5 mm], which exceed the maximum acceptable concentration of Quebec regulation of 1.0 mg/L. Zinc is highly mobile under near-neutral pH conditions, and its mobility is increasing as pH is decreasing (Cravotta 2008).

Calcium and magnesium mostly originated from the dissolution of carbonates and possibly, to a lower extent, of silicates such as anorthite ($CaAl_2Si_2O_8$), actinolite ($Ca_2(Mg,Fe)_5Si_8O_{22}(OH)_2$). Calcium and magnesium concentrations from the large columns were doubled in C6 (70 mg/L and 2 mg/L, respectively) compared to the coarse fraction C5 (35 mg/L and 1 mg/L). The concentration of calcium was greater in the fine fraction C1 (700 mg/L), followed by the fraction C2 (40 mg/L) > C3 (30 mg/L) > C4 (20 mg/L), suggesting that there is a greater carbonate dissolution from the fines. The same trend with fraction size was observed for magnesium concentrations (Fig. 9f).

In summary, the pH decreased gradually but remained around neutrality in all the columns, despite the acid-generating potential of all fractions (Fig. 6e). The steady concentrations of calcium and magnesium measured in the leachates indicate that neutralization processes may have been able to maintain the pH near neutrality and that carbonates were not depleted yet at the end of the column tests. Similar to CM waste rock, sulfate concentrations were the highest in the fine fraction C1 [0; 1 mm] and in the whole fraction C6 [0; 37.5 mm], indicating that the fine fractions had the most influence on oxidation processes. Calcium and magnesium concentrations followed a similar pattern to a lesser extent, suggesting that the fine fractions also contributed more to the neutralization processes.

Results analysis and discussion

Effect of particle size and sulfur distribution on sulfate release rates

The cumulative mass-normalized sulfate release rates were used to compare column results from different scales (Bouzahzah et al. 2014). Cumulative mass-normalized sulfate release rates were calculated from the fifth cycle (using linear regression) when the geochemical behavior was stabilized, to ensure that the sulfate release rates were indicative of sulfide weathering rates and not from the dissolution of prior products (Plante et al. 2011). The reaction products (here sulfates) were assumed entirely flushed in the leachate and not retained as secondary minerals salts. Simulations conducted with VMINTEQ after the fifth cycle showed that saturation indexes were negative for secondary products of sulfates (e.g., gypsum, jarosite), thus confirming the assumption of sulfate products (e.g., ranging between − 1.2 and − 3.2 for gypsum in all columns; for more details, see Supplementary data).

The sulfate release rate in fraction C1 (mg/kg/day) consistently exceeded the rates in fractions C2 to C5 (Table 1). More specifically, the release rates of the fractions of CM and LR followed the order: C1 > C2 > C3 > C4 > C5. In the case of CM waste rock, where sulfur distribution did not significantly change with fraction size (∼ 2%), the normalized sulfate release rate was greater in C1 (9.5 mg/kg/day) compared to C2 to C5 (0.2–1.2 mg/kg/day), by an order of magnitude. Consequently, particle size was controlling the sulfide weathering rate due to their liberation (exposure). Specifically, fraction C1 [0; 1.00 mm] of LR waste rock was enriched in sulfur (∼ 6%), in comparison to all the other fractions C2 to C5 (∼ 3%). The sulfate release rate was more than one order of magnitude greater in C1 (44.6 mg/kg/day) compared to C2 to C5 (0.6–1.1 mg/kg/day). Therefore, the sulfate release rates were controlled by particle size to a greater extent, but also by sulfur content distribution.

Table 1 Cumulative normalized to mass sulfate release rates and normalized to mass of S

Laboratory columns	CM		LR	
	Cumulative normalized sulfate release rates (mg/kg/day)	Cumulative normalized to S sulfate release rates (mg/kg S/day)	Cumulative normalized sulfate release rates (mg/kg/day)	Cumulative normalized to S sulfate release rates (mg/kg S/day)
C1 [0; 1.00 mm]	9.5	528	42.9	681
C2 [1; 2.36 mm]	1.0	91	1.1	37
C3 [2.36; 3.35 mm]	0.4	24	0.9	30
C4 [3.35; 4.75 mm]	0.4	29	0.8	27
C5 [4.75; 37.5 mm]	0.1	5	0.6	21
C6 [0; 37.5 mm]	1.2	67	1.6	42

**Table 2** Cumulative normalized sulfate release rates in the small and large cells and prediction

Fractions	Cumulative normalized sulfate release rates (mg/kg/day)	
	CM	LR
C6 [0; 37.5 mm] estimated	2.2	8.9
C1–C4 [0; 4.75 mm] estimated	2.2	8.5
C6 [0; 37.5 mm] measured	1.2	1.6

Sulfate release rates were also normalized with sulfur content to allow comparison of CM and LR waste rock. The observed rate in fraction C1 was greater in the LR waste rock (681 mg/kg of S/day) in comparison to CM waste rock (528 mg/kg of S/day). This variation can be attributed to distinct intrinsic characteristics of the mineralogy such as different specific surface areas of the fraction C1 (i.e., the crystal size of the pyrite or the crystal type; Evangelou and Zhang 1995), a possible galvanic effect at the interfaces between pyrite and chalcopyrite or sphalerite in LR waste rock, where chalcopyrite and sphalerite were here only identified by mineral reconciliation (Kwong et al. 2003; St-Arnault et al. 2020), or variations in the degree of liberation of the sulfide minerals between the waste rock (Elghali et al. 2018; Mafra et al. 2020). In the coarse fractions, the cumulative sulfate release rates normalized to the mass of S did not show significant variations between fractions C2 to C5. For example, the sulfate release rates normalized with sulfur in LR waste rock had no significant change between C2 and C5 (37 to 21 mg/kg S/day). This could indicate a relatively similar sulfide exposition between these fractions. However, a significant change in the sulfate release rates normalized to pyrite was observed for CM

Fig. 7 Evolution of pH (**a**), sulfates (**b**), iron (**c**), zinc (**d**), calcium (**e**) and magnesium (**f**) concentrations in CM waste rock columns C1 to C4
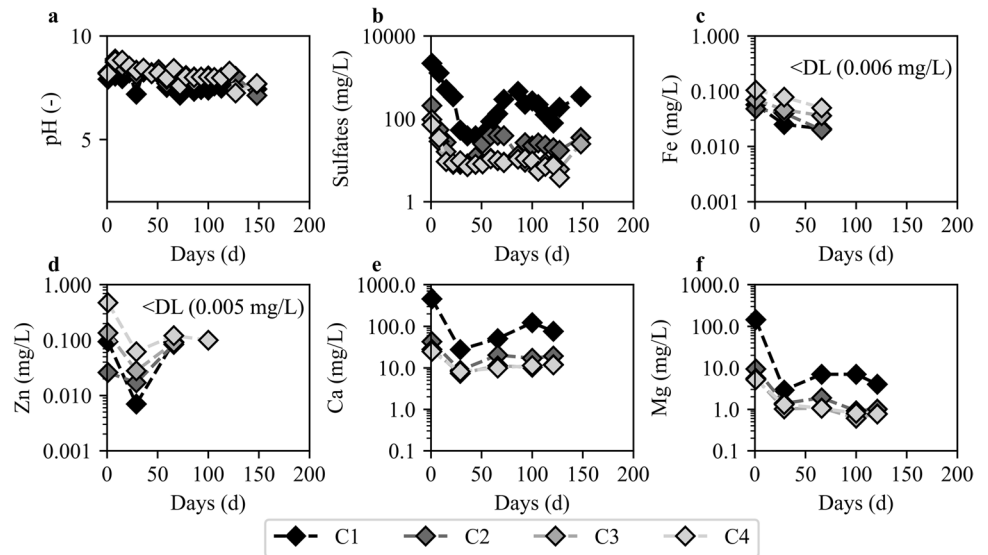
Fig. 8 Evolution of pH (**a**), sulfates (**b**), iron (**c**), zinc (**d**), calcium (**e**) and magnesium (**f**) concentrations in CM waste rock columns C5 and C6
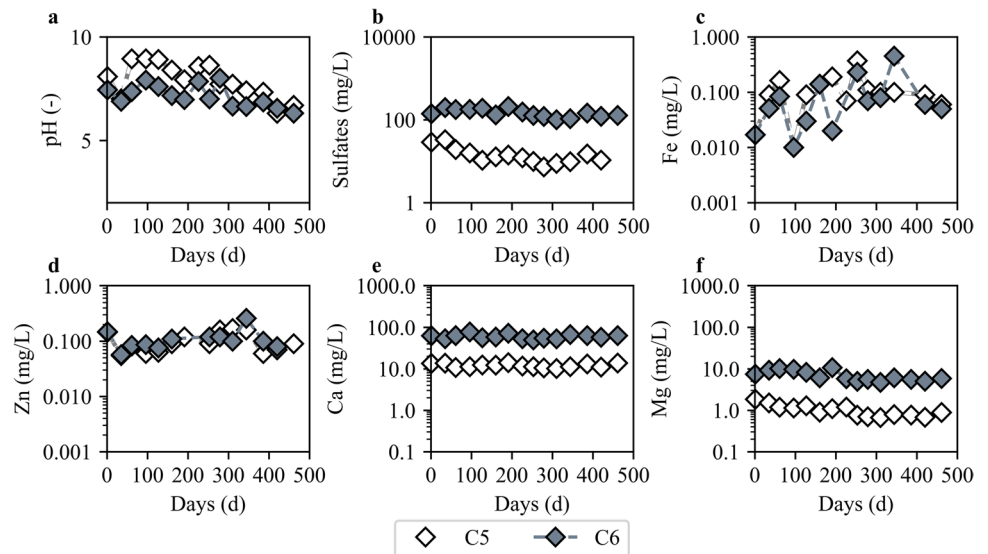
Fig. 9 Evolution of pH (**a**), sulfates (**b**), iron (**c**), zinc (**d**), calcium (**e**) and magnesium (**f**) concentrations in LR waste rock columns C1 to C4
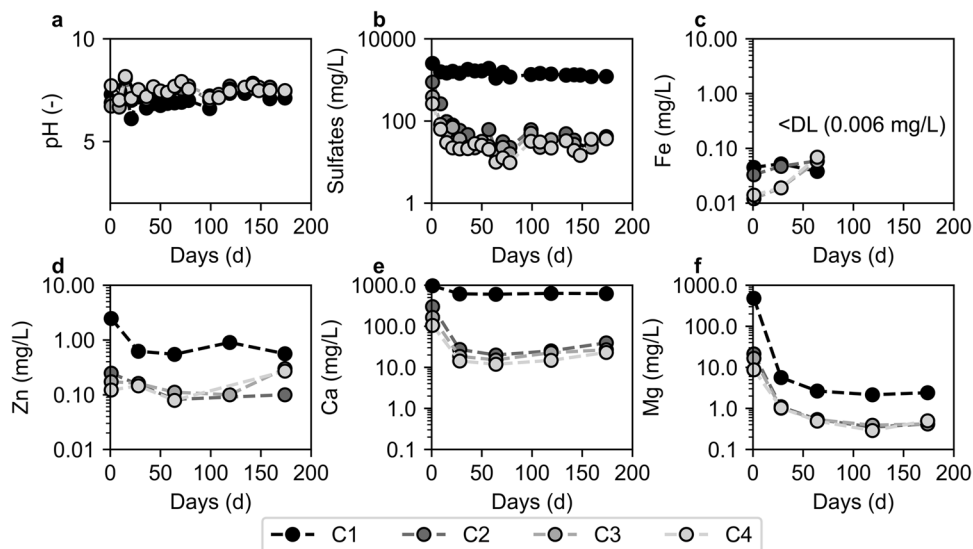
Fig. 10 Evolution of pH (**a**), sulfates (**b**), iron (**c**), zinc (**d**), calcium (**e**) and magnesium (**f**) concentrations in LR waste rock columns C5 and C6
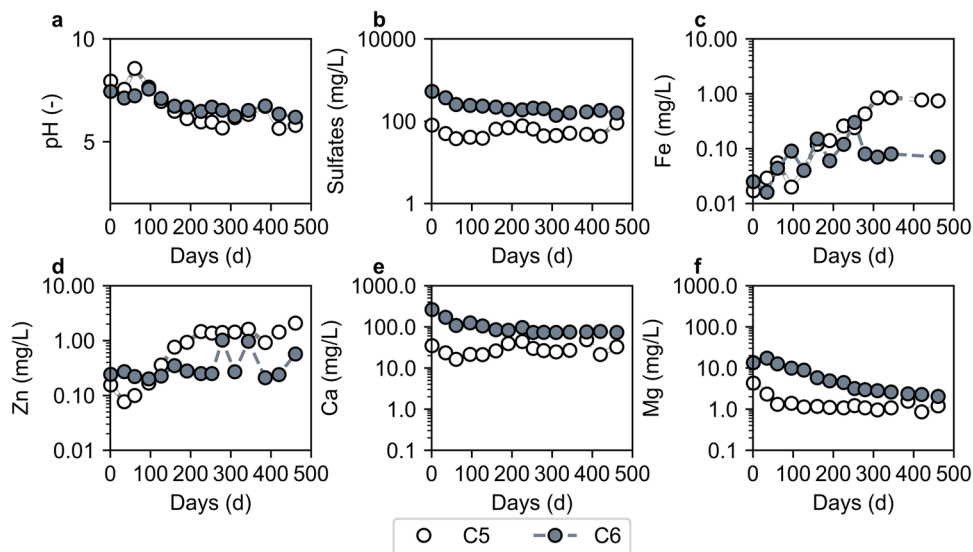
waste rock, which can be attributed to a significant decrease in the sulfide exposition when increasing particle size.

Overall, results indicated that particle size primarily controlled sulfate release rates. However, several other factors including sulfur distribution and mineralogy contributed to reactivity to a lesser extent. The sulfate release rates normalized to S showed a more significant decrease in CM compared to LR waste rock.

Scaling up and estimating overall reactivity using fractions at an intermediate scale

Results of each complementary waste rock fraction were used to predict the cumulative normalized sulfate release rates (mg/kg/day) of the entire waste rock sample with respect to its PSD. Specifically, the results from the complementary fractions C1 to C4 (small scale; 1 kg) and fraction

C5 (larger column; 55.3 kg) were combined using a sum of weight based on the particle size distribution curve (Table 2) and compared to C6 [0; 37.5 mm]. Calculated sulfate release rates for CM and LR were twice and six times greater, respectively, than the one measured in column C6. The contribution of the small fractions [0; 4.75 mm] accounted for more than 95% of the estimated reactivity, even if fraction [4.75; 37.5 mm] accounted for more than 60% of the total mass.

Prediction models for contaminant loads typically use laboratory experiments, such as humidity cells (ASTM D5744–18 2018) and/or kinetic column tests (Bouzahzah et al. 2014), to scale up to field results (Plante et al. 2014) and ultimately to full-scale waste storage facilities (Vriens et al. 2020a). However, the prediction of waste rock reactivity at a larger scale remained a great challenge given

the particle size exceeding 1 m and the impracticability of conducting laboratory test respecting such dimensions and column diameter ratio (e.g., ratio of 8 between maximum particle size and the diameter of a column). Testing the fine fraction, which is assumed to control AMD and impact more the geochemical behavior of waste rock, represents a conservative approach. Yet, there is no standard method for scaling laboratory release rates to larger particles and full-scale waste rock piles. The measured sulfate release rate is also sometimes normalized by the sulfur content and specific surface area, to predict water quality in waste rock at field scale (Vriens et al. 2020; Bailey et al. 2023;). Significant variations in estimated mass load, ranging from two to three orders of magnitude, were also observed, attributed to the lack of consideration for physical and mineralogical heterogeneity in humidity cell (Bailey et al. 2023). Large-scale experiments tend to yield lower mass loadings of contaminants compared to small-scale experiments such as kinetic column tests or humidity cells, even when dealing with similar waste rock (Vriens et al. 2020a). These differences are often attributed to the differences in water and liquid ratio, which can influence rate differences at varying scales (Plante et al. 2014) and the heterogeneity of the waste rock. In this research, the ratio of solid/liquid in the small weathering columns and the large columns was similar (~ 0.4). However, the size of the columns and the flushing rates and frequencies were different (small; weekly and large; monthly). Typically, lower flushing rates tend to increase secondary mineral precipitations, potentially reducing the mobility of reaction products (Sapsford et al. 2009). Furthermore, only by increasing column dimension, the sulfate release rates can be reduced (Erguler et al. 2014).

In summary, testing the small fractions (here C1 to C4) can help determine the contribution from specific fractions and define a potential diameter where the reactivity is decreasing. However, the use of the small fractions to predict the geochemical behavior of larger particles or whole waste rock can lead to overestimations of the reactivity. Laboratory results are sensitive to the flushing rates and frequencies, the solid/liquid ratio, the particle size, and the column dimensions (Erguler and Kalyoncu Erguler 2015).

Challenges in controlling AMD generation by sieving

In this study, increasing the fraction sizes proved beneficial in reducing the normalized sulfate release rate. In the estimation of the sulfate release rate, the fraction [0; 4.75 mm] accounted for more than 95% of the overall sulfate release rates. Sieving fine particles at 4.75 mm could therefore be beneficial to reduce the sulfate release rates (i.e., the oxidation and potential for AMD generation). Particularly, in CM waste rock, the sulfate release rate was 0.1 mg/kg/day in the

coarse fraction C5 [4.75; 37.5], whereas it reached 1.2 mg/kg/day (i.e., 12 times greater) in the total sample C6 [0; 37.5 mm] (Table 3), demonstrating promising outcomes for re-use potential. Similarly, within LR waste rock, the sulfate release rate in C6 (1.6 mg/kg/day) was three times greater than in C5 (0.5 mg/kg/day). While promising outcomes for re-use potential were observed in CM waste rock (e.g., low metal concentrations), the complexity of the physicochemical process in waste rock challenges the assumptions that coarser fractions inherently produce lower contaminant loads.

Several studies have demonstrated that contaminant loads do not systematically decrease with increasing particle sizes (Parbhakar-Fox et al. 2013). The contaminant loads can indeed be controlled by multiple physicochemical phenomena such as galvanic effects (Kwong et al. 2003), or precipitations of secondary minerals (Herbert 2003), and are highly specific to the studied material (Lapakko et al. 2006). In this study, sieving the fine fractions also showed effects on neutralization products, particularly regarding calcium and magnesium release rates (Table 3). For the studied waste rock, the total fraction C6 exhibited higher calcium and magnesium rates than the coarse fraction C5. This can be partly attributed to lower acid production as evidenced by the lower sulfate release rates of C5 for CM waste rock. However, the pH observed in LR leachates from C5 was slightly lower than the pH (Fig. 8b) from the total fraction C6. This could indicate that the fine fractions are likely to exert influence in pH neutralization, potentially impacting water quality as lower pH can increase the concentration of metals (e.g., iron) in the leachates (Cravotta III 2008). Carbonate minerals in the fine fraction [0; 4.75 mm] are likely more liberated compared to the coarser fraction, potentially influencing the neutralization processes in LR waste rock.

Sieving fine particles in LR waste rock resulted in higher zinc and iron release rates (Table 2), and higher metal concentrations (Fig. 10b and c) were observed in the LR C5 coarse fraction. Secondary mineral precipitations can control contaminant release rates (Jönsson et al. 2006). For example,

Table 3 Release rates of elements from sulfide mineral oxidation and neutralization minerals

	Release rates (mg/kg/day)			
	CM		LR	
	C5 [4.75; 37.5 mm]	C6 [0; 37.5 mm]	C5 [4.75; 37.5 mm]	C6 [0; 37.5 mm]
Sulfate	0.1	1.2	0.6	1.5
Iron	0.001	0.001	0.005	0.0008
Zinc	0.001	0.001	0.01	0.004
Calcium	0.1	0.5	0.3	0.7
Magnesium	0.008	0.05	0.01	0.03

precipitations of iron oxyhydroxide minerals can enhance sorption capacity and control metal concentrations (Biswas et al. 2022). For example, zinc tends to adsorb to lepidocrocite and other iron species (Herbert 2003). The geochemical speciation model performed on LR leachates revealed that there was no significant difference in the positive saturation indexes calculated between columns C5 and C6 for iron oxyhydroxides minerals (e.g., goethite, lepidocrocite, ferrihydrite). Additionally, simulations showed that no secondary zinc mineral phases were expected to precipitate (negative saturation index) under the measured temperature, Eh, and pH conditions in both columns C5 and C6. Therefore, secondary mineral precipitations, specifically iron oxyhydroxides, were identified as controlling factors for zinc concentrations in LR leachates. The observed higher sulfate release rates in C6 (three times greater than C5) suggested a proportional release of iron (i.e., pyrite oxidation products of 2 mol of sulfates and 1 mol of iron), and thus, because pH was near neutrality, a greater formation of iron precipitate retained in the column C6. Therefore, zinc adsorption was assumed to be greater in C6 than in C5, which was also confirmed by a lower concentration of zinc in the C6 leachates. However, the stability of zinc adsorbed on precipitates in C6 can remain a significant concern, as a slight decrease in pH may result in a substantial release of zinc from the solid (Jönsson et al. 2006).

In general, the sulfate release rates were significantly reduced in the coarse fraction C5 than in the fraction C6 for the studied waste rock, suggesting a potential improvement in water quality. Nevertheless, the neutralization processes in the LR waste rocks were unable to stabilize pH, resulting in a progressive decrease over time and an increase in metal concentrations for both fractions (Fig. 10). Secondary mineral precipitations can be the main process controlling zinc concentrations.

Potential for developing circular economy approaches

The results of this research have shown that the sieving of reactive waste rock represents a promising strategy for circular economy approaches by separating a non-reactive coarse fraction and a more reactive fine fraction. The fraction for re-use could be determined using kinetic tests by fractions, such as previously described in this study. Alternative characterization techniques such as automated mineralogy and computed tomography could also complement kinetic tests to optimize the selection of the critical diameter of re-use (Elghali et al. 2018, 2019; Ait-khouia et al. 2023). Potential applications within the mining industry include the use of non-reactive waste rock in cover systems for reclamation purposes, such as an evaporation barrier (Pabst et al. 2018; Sylvain et al. 2019), or in civil engineering, such as

the production of concretes amended with mine waste (Taha et al. 2021). The remaining non-reactive waste rock could be stored in piles, separately from the reactive fine fractions, thus reducing both the size of the storage facilities and the cost of reclamation.

The separated reactive fine fractions of waste rock could be desulfurized similar to tailings (Amar et al. 2020). Such an approach is usually not applicable to waste rock (Demers and Pabst 2021) but could be adapted to the fine fraction of waste rock, provided the maximum particle size does not exceed 10 mm for most operation units for physical separation techniques (which was the case in this study) (Amar et al. 2021; Masindi et al. 2022). The non-reactive fine waste rock could be re-used in cover systems for reclamation purposes similar to tailings (Rey et al. 2016; Kalonji Kabambi et al. 2017; Demers and Pabst 2021). The separation of the coarse and the fine fractions of waste rock, combined with innovative desulfurization and recovery processes of the fines, and their re-use in various applications, would significantly reduce (and potentially completely eliminate) the volume of mine waste that needs to be disposed of on the surface and reclaimed, enhance resource utilization, and decrease the footprint associated with waste disposal (Ait-Khouia et al. 2021).

Discussion

In this study, only two types of waste rock with similar PSD but different geochemical characteristics were used. The results showed the importance of mineralogy on the geochemical behavior, and more waste rock should be tested as the potential of re-use of waste rock is site-specific. This study was performed on a small and intermediate scale; however, geochemical behavior tends to differ from a larger scale in the field due to the liquid/solid ratio (Plante et al. 2011), the particle size (which can reach 1 m at the field scale), precipitation/dissolution of secondary minerals (Vriens et al. 2020), sorption phenomena (Plante et al. 2010), and temperature (Bailey et al. 2023). Standard static tests did not reveal any significant reduction in the NP between the fractions C5 and C6 for both waste rock (e.g., 22 and 26 kg $CaCO_3$/ton in C5 and C6 for LR, respectively; Table A.1). The same observation was made for the AP between fractions C5 and C6 for CM (43 kg $CaCO_3$/ton and 48 kg $CaCO_3$/ton in C5 and C6). Static tests assume complete liberation of both C and S, leading to inadequate assessment of the impact of sieving the fine fraction on the potential for acid generation, particularly for coarse particles.

The saturation index for gypsum calculated using VMINTEQ was negative, therefore indicating no (or very limited) precipitation (also see Supplementary data). The precipitation of gypsum is more frequently observed in column tests compared to humidity cells due to the quantity

of water and the flush frequency (Morin and Hutt 1998). The column tests were conducted on waste rock that did not generate acid prior to testing. Pre-oxidized waste rock may be the only material available on-site for re-use. Future work involves conducting column tests on material that is already generating acidity. Sieving of the fine fractions could be beneficial for the water quality. However, some uncertainties remained unclear regarding the presence of secondary minerals or acid salts, such as jarosite, which could dissolve and consequently sustain acid generation in the absence of sulfide oxidation (Nordstrom and Alpers 1999).

Conclusion

This experiment investigated the potential of re-use of two acid-generating waste rocks by controlling the particle size (sieving) to reduce the reactivity. Static and kinetic tests were performed for six fractions, and fraction [0; 1.00 mm] showed the highest sulfate release rates for all the waste rocks studied. Particle size predominantly influenced the sulfate release rates, which was decreasing as particle size increased for both waste rocks [0; 1.00 mm] > [1.00; 2.36 mm] > [2.36; 3.35 mm] > [3.35; 4.75 mm] > [4.75; 37.5 mm]. This reduction was predominantly attributed to the particle size (i.e., degree of liberation of the sulfides) but also the distribution of the sulfide minerals (e.g., greater content of sulfide minerals in LR sample [0–1 mm]). Therefore, static and kinetic testing of waste rock should be done by a fraction to fully identify the contribution of fractions on the overall reactivity.

The combined cumulative sulfate release rates of the small columns C1 to C4 [0; 4.75 mm] and the large columns C5 [4.75; 37.5 mm] to predict the rates of the total sample [0; 37.5 mm] were performed, and the cumulative sulfate release rates were overestimated. Extrapolate results from small-scale tests [0; 4.75 mm] to assess waste rock behavior for larger fractions remained a challenge, yet this approach remained conservative.

The present study also highlighted the importance of sieving the fine particles [0; 4.75 mm] of reactive waste rock to reduce the risks of acidic effluent from the whole waste rock mass. The coarser particle sizes C5 [4.75; 37.5 mm] showed lower sulfate release rates than the total sample C6 [0; 37.5 mm] in the studied waste rocks. However, the complexity of physicochemical processes such as liberation of the carbonate minerals and secondary mineral precipitations in waste rock challenges the assumption that coarser fraction inherently shows lower contaminant loads. A thorough geochemical characterization by fractions specific to each waste rock remains therefore strongly relevant for many studies. Further research in this direction holds promise for cost-effective management of reactive waste rock, with the potential to selectively reduce contaminant load, thus contributing to the emergence of novel sustainable practices.

Author contribution All authors contributed to the study conception, methodology, and analysis. Material preparation, data collection, and analysis were performed by Karine Sylvain. The first draft of the manuscript was written by Karine Sylvain, and all authors commented and edited on previous versions of the manuscript. The supervision, the resources, the funding acquisition, and the validation of the research were done by Thomas Pabst and Isabelle Demers. All authors read and approved the final manuscript.

Data availability The datasets used and/or analyzed in this study can be obtained from the corresponding author upon reasonable request.

Declarations

Ethical approval Not applicable.

Consent to participate Not applicable.

Consent for publication Not applicable.

Competing interests The authors declare no competing interests.

References

Agnico Eagle (2021) Mise à jour du plan de restauration - LaRonde et Bousquet 2. Ministère des Ressources naturelles et des Forêts Québec.

Ait-Khouia Y, Benzaazoua M, Demers I (2021) Environmental desulfurization of mine wastes using various mineral processing techniques: recent advances and opportunities. Miner Eng 174:107225. https://doi.org/10.1016/j.mineng.2021.107225

Ait-khouia Y, Benzaazoua M, Ievgeniia M, Demers I (2023) Moving towards sustainable mine waste rock management through automated mineral and geochemical analysis. J Geochem Explor 248:107182. https://doi.org/10.1016/j.gexplo.2023.107182

Alam R, Shang JQ (2012) Effect of operating parameters on desulphurization of mine tailings by froth flotation. J Environ Manage 97:122–130. https://doi.org/10.1016/j.jenvman.2011.11.013

Amar H, Benzaazoua M, Elghali A, Bussière B, Duclos M (2020) Upstream environmental desulphurisation and valorisation of waste rocks as a sustainable AMD management approach. J Geochem Explor 215:106555. https://doi.org/10.1016/j.gexplo.2020.106555

Amar H, Benzaazoua M, Edahbi M, Villeneuve M, Joly M-A, Elghali A (2021) Reprocessing feasibility of polymetallic waste rock for cleaner and sustainable mining. J Geochem Explor 220:106683. https://doi.org/10.1016/j.gexplo.2020.106683

Amos RT, Blowes DW, Bailey BL, Sego DC, Smith L, Ritchie AIM (2015) Waste-rock hydrogeology and geochemistry. Appl Geochem 57:140–156. https://doi.org/10.1016/j.apgeochem.2014.06.020

ASTM C127–15 (2015) Standard test method for relative density (specific gravity) and absorption of coarse aggregate. ASTM International, West Conshohocken, PA. www.astm.org

ASTM C702/C702M-18 (2018) Standard practice for reducing samples of aggregate to testing size. ASTM International, West Conshohocken, PA. www.astm.org

ASTM D5744–18 (2018) Standard test method for laboratory weathering of solid materials using a humidity cell. ASTM International, West Conshohocken, PA. www.astm.org

ASTM D6913/D6913M-17 (2021) Standard test methods for particle-size distribution (gradation) of soils using sieve analysis. ASTM International, West Conshohocken, PA. www.astm.org

ASTM D854–14 (2014) Standard test methods for specific gravity of soil solids by water pycnometer. ASTM International, West Conshohocken, PA. www.astm.org

Aubertin M (2013) Waste rock disposal to improve the geotechnical and geochemical stability of piles. Proc., 23rd World Mining Congress. Montréal, Québec

Aznar-Sánchez JA, García-Gómez JJ, Velasco-Muñoz JF, Carretero-Gómez A (2018) Mining waste and its sustainable management: advances in worldwide research. Minerals 8(7):284. https://doi.org/10.3390/min8070284

Bailey BL, Amos RT, Blowes DW, Moore ML, Ptacek CJ, Smith L, Sego DC (2023) Diavik waste-rock project, Northwest Territories, Canada: predicting field-scale waste-rock drainage quality from humidity-cell experiments. Econ Geol 118(3):585–597. https://doi.org/10.5382/econgeo.4932

Bao Z, Blowes DW, Ptacek CJ, Bain J, Holland SP, Wilson D, MacKenzie P (2020) Faro waste rock project: characterizing variably saturated flow behavior through full-scale waste-rock dumps in the continental subarctic region of Northern Canada using field measurements and stable isotopes of water. Water Resources Research 56(3):e2019WR026374. https://doi.org/10.1029/2019WR026374

Benzaazoua M, Kongolo M (2003) Physico-chemical properties of tailing slurries during environmental desulphurization by froth flotation. Int J Miner Process 69(1–4):221–234. https://doi.org/10.1016/S0301-7516(02)00129-1

Biswas A, Hendry MJ, Essilfie-Dughan J, Day S, Villeneuve SA, Barbour SL (2022) Geochemistry of zinc and cadmium in coal waste rock, Elk Valley, British Columbia Canada. Appl Geochem 136:105148. https://doi.org/10.1016/j.apgeochem.2021.105148

Blackmore S, Vriens B, Sorensen M, Power IM, Smith L, Hallam SJ, Beckie RD (2018) Microbial and geochemical controls on waste rock weathering and drainage quality. Sci Total Environ 640:1004–1014. https://doi.org/10.1016/j.scitotenv.2018.05.374

Blowes DW, Ptacek CJ, Jambor JL, Weisener CG (2014) The geochemistry of acid mine drainage. In: Treatise on geochemistry, pp 149–204. https://doi.org/10.1016/B0-08-043751-6/09137-4

Bouzahzah H, Benzaazoua M, Bussiere B, Plante B (2014) Prediction of acid mine drainage: importance of mineralogy and the test protocols for static and kinetic tests. Mine Water Environ 33(1):54–65. https://doi.org/10.1007/s10230-013-0249-1

Chi X, Amos RT, Stastna M, Blowes DW, Sego DC, Smith L (2013) The Diavik Waste Rock Project: implications of wind-induced gas transport. Appl Geochem 36:246–255. https://doi.org/10.1016/j.apgeochem.2012.10.015

Clesceri L, Greenberg A,Eaton A (1998) Method no. 4500-SO4 2E. Turbidimetric method: sulfate. Standard Methods for the Examination of Water and Waste Water, 4–178.

Cravotta III CA (2008) Dissolved metals and associated constituents in abandoned coal-mine discharges, Pennsylvania, USA. Part 2: geochemical controls on constituent concentrations. Applied Geochemistry, 23(2), 203–226. https://doi.org/10.1016/j.apgeochem.2007.10.003

Demers I and Pabst T (2021) Alternative and innovative integrated mine waste management approaches. In: Hard Rock Mine Reclamation: From Prediction to Management of Acid Mine Drainage. https://doi.org/10.1201/9781315166698

Derycke V, Kongolo M, Benzaazoua M, Mallet M, Barrès O, De Donato P, Mermillod-Blondin R (2013) Surface chemical characterization of different pyrite size fractions for flotation purposes. Int J Miner Process 118:1–14. https://doi.org/10.1016/j.minpro.2012.10.004

Dimech A, Cheng L, Chouteau M, Chambers J, Uhlemann S, Wilkinson P, Isabelle A (2022) A review on applications of time-lapse electrical resistivity tomography over the last 30 years: perspectives for mining waste monitoring. Surveys in Geophysics, 1–61. https://doi.org/10.1007/s10712-022-09731-2

Elghali A, Benzaazoua M, Bouzahzah H, Bussière B, Villarraga-Gómez H (2018) Determination of the available acid-generating potential of waste rock, part I: Mineralogical approach. Appl Geochem 99:31–41. https://doi.org/10.1016/j.apgeochem.2018.10.021

Elghali A, Benzaazoua M, Bussière B, Bouzahzah H (2019) Determination of the available acid-generating potential of waste rock, part II: Waste management involvement. Appl Geochem 100:316–325. https://doi.org/10.1016/j.apgeochem.2018.12.010

Erguler ZA, Erguler GK (2015) The effect of particle size on acid mine drainage generation: kinetic column tests. Miner Eng 76:154–167. https://doi.org/10.1016/j.mineng.2014.10.002

Erguler GK, Erguler ZA, Akcakoca H, Ucar A (2014) The effect of column dimensions and particle size on the results of kinetic column test used for acid mine drainage (AMD) prediction. Miner Eng 55:18–29. https://doi.org/10.1016/j.mineng.2013.09.008

Evangelou VP, Zhang Y (1995) A review: pyrite oxidation mechanisms and acid mine drainage prevention. Crit Rev Environ Sci Technol 25(2):141–199. https://doi.org/10.1080/10643389509388477

Fala O, Molson J, Aubertin M, Dawoo I, Bussière B, Chapuis R (2013) A numerical modelling approach to assess long-term unsaturated flow and geochemical transport in a waste rock pile. Int J Min Reclam Environ 27(1):38–55. https://doi.org/10.1080/17480930.2011.644473

Fala O, Aubertin M, Molson J, Bussière B, Wilson GW, Chapuis R, Martin V (2003) Numerical modelling of unsaturated flow in uniform and heterogeneous waste rock piles. Sixth International Conference on Acid Rock Drainage (ICARD), Australasian Institute

of Mining and Metallurgy, vol 3, Cairns, Australia, Publication Series, pp 895–902

Fredlund MD, Fredlund D, Wilson GW (2000) An equation to represent grain-size distribution. Can Geotech J 37(4):817–827. https://doi.org/10.1139/t00-015

Helt KM, Williams-Jones AE, Clark JR, Wing BA, Wares RP (2014) Constraints on the genesis of the archean oxidized, intrusion-related canadian malartic gold deposit, Quebec Canada. Econ Geol 109(3):713–735. https://doi.org/10.2113/econgeo.109.3.713

Herbert RB (2003) Zinc immobilization by zerovalent Fe: surface chemistry and mineralogy of reaction products. Mineral Mag 67(6):1285–1298. https://doi.org/10.1180/0026461036760165

Hollings P, Hendry M, Nicholson R, Kirkland R (2001) Quantification of oxygen consumption and sulphate release rates for waste rock piles using kinetic cells: Cluff lake uranium mine, northern Saskatchewan Canada. Appl Geochem 16(9–10):1215–1230. https://doi.org/10.1016/S0883-2927(01)00005-1

Jambor JL, Ptacek CJ, Blowes DW, Moncur MC (2005) Acid drainage from the oxidation of iron sulfides and sphalerite in mine wastes. Proceedings of Lead & Zinc '05, vol 1, The Mining and Materials Processing Institute of Japan, pp 715–737

James M, Aubertin M, Bussière B (2013) On the use of waste rock inclusions to improve the performance of tailings impoundments. Proceedings of the 18th International Conference Soil Mechanics and Geotechnical Engineering, Paris, France, pp 2–6

Jönsson J, Jönsson J, Lövgren L (2006) Precipitation of secondary Fe (III) minerals from acid mine drainage. Appl Geochem 21(3):437–445. https://doi.org/10.1016/j.apgeochem.2005.12.008

Kalonji Kabambi A, Bussière B, Demers I (2017) Hydrogeological behaviour of covers with capillary barrier effects made of mining materials. Geotech Geol Eng 35(3):1199–1220. https://doi.org/10.1007/s10706-017-0174-3

Kwong YJ, Swerhone GW, Lawrence JR (2003) Galvanic sulphide oxidation as a metal-leaching mechanism and its environmental implications. Geochem: Explor Environ Anal 3(4):337–343. https://doi.org/10.1144/1467-7873/03/013

Lahmira B, Lefebvre R, Hockley D, Phillip M (2014) Atmospheric controls on gas flow directions in a waste rock dump. Vadose Zone J 13(10):1–17. https://doi.org/10.2136/vzj2014.03.0032

Lahmira B, Lefebvre R, Aubertin M, Bussière B (2016) Effect of heterogeneity and anisotropy related to the construction method on transfer processes in waste rock piles. J Contam Hydrol 184:35–49. https://doi.org/10.1016/j.jconhyd.2015.12.002

Lahmira B, Lefebvre R, Aubertin M, Bussière B (2017) Effect of material variability and compacted layers on transfer processes in heterogeneous waste rock piles. J Contam Hydrol 204:66–78. https://doi.org/10.1016/j.jconhyd.2017.07.004

Lapakko KA, Engstrom JN, Antonson DA (2006) Effects of particle size on drainage quality from three lithologies. Poster paper presented at the 7th International Conference on Acid Rock Drainage (ICARD) (pp. 1026–1050).

Laverdière A, Hao S, Pabst T, Courcelles B (2023) Effect of gradation, compaction and water content on crushed waste rocks strength. Road Mater Pavement Design 24(3):761–775. https://doi.org/10.1080/14680629.2022.2044373

Li M, Zhang J, Song W, Germain DM (2019) Recycling of crushed waste rock as backfilling material in coal mine: effects of particle size on compaction behaviours. Environ Sci Pollut Res 26:8789–8797. https://doi.org/10.1007/s11356-019-04379-9

Mafra C, Bouzahzah H, Stamenov L, Gaydardzhiev S (2020) Insights on the effect of pyrite liberation degree upon the acid mine drainage potential of sulfide flotation tailings. Appl Geochem 123:104774. https://doi.org/10.1016/j.apgeochem.2020.104774

Marescotti P, Azzali E, Servida D, Carbone C, Grieco G, De Capitani L, Lucchetti G (2010) Mineralogical and geochemical spatial analyses of a waste-rock dump at the Libiola Fe–Cu sulphide mine (Eastern Liguria, Italy). Environ Earth Sci 61(1):187–199. https://doi.org/10.1007/s12665-009-0335-7

Martin V, Bussière B, Plante B, Pabst T, Aubertin M, Medina F, Poaty B. (2017) Controlling water infiltration in waste rock piles: design, construction, and monitoring of a large-scale in-situ pilot test pile. Proceedings of the 70th Canadian Geotechnical Society Conference (Vol. 70).

Masindi V, Foteinis S, Renforth P, Ndiritu J, Maree J, Tekere M, Chatzisymeon E (2022) Challenges and avenues for acid mine drainage treatment, beneficiation, and valorisation in circular economy: a review. Ecol Eng 183:106740. https://doi.org/10.1016/j.ecoleng.2022.106740

Mine Canadian Malartic (2020) Plan de restauration - Révision 3. Ministère des Ressources naturelles et des Forêts Québec. https://gestim.mines.gouv.qc.ca/

Molson J, Fala O, Aubertin M, Bussière B (2005) Numerical simulations of pyrite oxidation and acid mine drainage in unsaturated waste rock piles. J Contam Hydrol 78(4):343–371. https://doi.org/10.1016/j.jconhyd.2005.06.005

Morin KA and Hutt NM (1998) Kinetic tests and risk assessment for ARD. In: 5th annual BC metal leaching and ARD workshop.9–10 Dec 1998, Vancouver, pp. 1–10.

Munroe EA, McLemore VT, Kyle P (1999) Waste rock pile characterization, heterogeneity, and geochemical anomalies in the Hillsboro Mining District, Sierra County, New Mexico. J Geochem Explor 67(1–3):391–405. https://doi.org/10.1016/S0375-6742(99)00068-0

Neuner M, Smith L, Blowes DW, Sego DC, Smith LJ, Fretz N, Gupton M (2013) The Diavik waste rock project: water flow through mine waste rock in a permafrost terrain. Appl Geochem 36:222–233. https://doi.org/10.1016/j.apgeochem.2012.03.011

Nordstrom DK, Alpers CN (1999) Negative pH, efflorescent mineralogy, and consequences for environmental restoration at the Iron Mountain Superfund site, California. Proc Natl Acad Sci 96(7):3455–3462. https://doi.org/10.1073/pnas.96.7.3455

Nordstrom DK, Blowes DW, Ptacek CJ (2015) Hydrogeochemistry and microbiology of mine drainage: an update. Appl Geochem 57:3–16. https://doi.org/10.1016/j.apgeochem.2015.02.008

Pabst T, Molson J, Aubertin M, Bussière B (2017) Reactive transport modelling of the hydro-geochemical behaviour of partially oxidized acid-generating mine tailings with a monolayer cover. Appl Geochem 78:219–233. https://doi.org/10.1016/j.apgeochem.2017.01.003

Pabst T, Bussière B, Aubertin M, Molson J (2018) Comparative performance of cover systems to prevent acid mine drainage from pre-oxidized tailings: a numerical hydro-geochemical assessment. J Contam Hydrol 214:39–53. https://doi.org/10.1016/j.jconhyd.2018.05.006

Parbhakar-Fox A, Lottermoser B, Bradshaw D (2013) Evaluating waste rock mineralogy and microtexture during kinetic testing for improved acid rock drainage prediction. Miner Eng 52:111–124. https://doi.org/10.1016/j.mineng.2013.04.022

Peregoedova A (2012) Étude expérimentale des propriétés hydrogéologiques des roches stériles à une échelle intermédiaire de laboratoire, École Polytechnique de Montréal

Plante B, Benzaazoua M, Bussière B, Biesinger M, Pratt A (2010) Study of Ni sorption onto Tio mine waste rock surfaces. Appl Geochem 25(12):1830–1844. https://doi.org/10.1016/j.apgeochem.2010.09.010

Plante B, Benzaazoua M, Bussière B (2011) Predicting geochemical behaviour of waste rock with low acid generating potential using laboratory kinetic tests. Mine Water Environ 30:2–21. https://doi.org/10.1007/s10230-010-0127-z

Plante B, Bussière B, Benzaazoua M (2014) Lab to field scale effects on contaminated neutral drainage prediction from the Tio mine waste rocks. J Geochem Explor 137:37–47. https://doi.org/10.1016/j.gexplo.2013.11.004

Price W (2009) Prediction manual for drainage chemistry from sulphidic geologic materials. Canadian MEND Report 1.20. 1, dated December 2009. Natural Resources Canada

Rey NJ, Demers I, Bussière B, Mbonimpa M, Lortie S (2016) Field experiments to test the elevated water table concept combined with a desulfurized tailings cover layer. In Geo-Chicago 2016 (pp. 289–298). https://doi.org/10.1061/9780784480137.029

Saleh-Mbemba F, Aubertin M, Boudrias G (2019) Drainage and consolidation of mine tailings near waste rock inclusions. In: Sustainable and Safe Dams Around the World/Un monde de barrages durables et sécuritaires. pp. 3296–3305.

Sapsford DJ, Bowell R, Dey M, Williams KP (2009) Humidity cell tests for the prediction of acid rock drainage. Miner Eng 22(1):25–36. https://doi.org/10.1016/j.mineng.2008.03.008

Smith LJ, Bailey BL, Blowes DW, Jambor JL, Smith L, Sego DC (2013a) The Diavik Waste Rock Project: initial geochemical response from a low sulfide waste rock pile. Appl Geochem 36:210–221. https://doi.org/10.1016/j.apgeochem.2012.06.008

Smith LJ, Blowes DW, Jambor JL, Smith L, Sego DC, Neuner M (2013b) The Diavik Waste Rock Project: particle size distribution and sulfur characteristics of low-sulfide waste rock. Appl Geochem 36:200–209. https://doi.org/10.1016/j.apgeochem.2013.05.006

St-Arnault M, Vriens B, Blaskovich R, Aranda C, Klein B, Mayer KU, Beckie RD (2020) Geochemical and mineralogical assessment of reactivity in a full-scale heterogeneous waste-rock pile. Min Eng 145:106089. https://doi.org/10.1016/j.mineng.2019.106089

Strömberg Band Banwart S (1999) Weathering kinetics of waste rock from the Aitik copper mine, Sweden: scale dependent rate factors and pH controls in large column experiments. J Contam Hydrol 39(1–2):59–89. https://doi.org/10.1016/S0169-7722(99)00031-5

Sylvain K, Pabst T, Dimech A (2019) Waste rock valorization in monolayer covers with elevated water table. Proceedings of GeoEnvironmental Engineering, pp 101–112

Taha Y, Benarchid Y, Benzaazoua M (2021) Environmental behavior of waste rocks based concrete: leaching performance assessment. Resour Policy 74:101419. https://doi.org/10.1016/j.resourpol.2019.101419

Tayebi-Khorami M, Edraki M, Corder G, Golev A (2019) Re-thinking mining waste through an integrative approach led by circular economy aspirations. Minerals 9(5):286. https://doi.org/10.3390/min9050286

Thompson R, Peroni R, Visser A (2019) Mining haul roads: theory and practice. CRC Press, Boca Raton. https://doi.org/10.1201/9780429491474

Vriens B, Peterson H, Laurenzi L, Smith L, Aranda C, Mayer KU, Beckie RD (2019a) Long-term monitoring of waste-rock weathering at the Antamina mine, Peru. Chemosphere 215:858–869. https://doi.org/10.1016/j.chemosphere.2018.10.105

Vriens B, Smith L, Mayer KU, Beckie RD (2019b) Poregas distributions in waste-rock piles affected by climate seasonality and physicochemical heterogeneity. Appl Geochem 100:305–315. https://doi.org/10.1016/j.apgeochem.2018.12.009

Vriens B, Plante B, Seigneur N, Jamieson H (2020a) Mine waste rock: insights for sustainable hydrogeochemical management. Minerals 10(9):728. https://doi.org/10.3390/min10090728

Vriens B, Seigneur N, Mayer KU, Beckie RD (2020) Scale dependence of effective geochemical rates in weathering mine waste rock. J Contam Hydrol 234:103699. https://doi.org/10.1016/j.jconhyd.2020.103699

Wilson D, Smith L, Atherton C, Smith LJ, Amos RT, Barsi DR, Blowes DW (2022) Diavik Waste Rock Project: geostatistical analysis of sulfur, carbon, and hydraulic conductivity distribution in a large-scale experimental waste rock pile. Minerals 12(5):577. https://doi.org/10.3390/min12050577